

Site-selective formation of Si nanocrystal in SiO₂ by femtosecond laser irradiation and Al deoxidization effects

Noriyuki Uchida,^{1,a)} Youhei Mikami,¹ Hiroshi Kintoh,¹ Kouichi Murakami,¹ Naoki Fukata,² Masanori Mitome,³ Muneaki Hase,^{1,4} and Masahiro Kitajima⁴

¹*Institute of Applied Physics, University of Tsukuba, 1-1-1 Tennoudai, Tsukuba, Ibaraki 305-8573, Japan*

²*International Center for Materials Nanoarchitectonics, National Institute for Materials Science, 1-1 Namiki, Tsukuba 305-0044, Japan and PRESTO, Japan Science and Technology (JST), 4-1-8 Honcho Kawaguchi, Saitama 332-0012, Japan*

³*Advanced Materials Laboratory, National Institute for Materials Science, 1-1 Namiki, Tsukuba, Ibaraki 305-0044, Japan*

⁴*Advanced Nano Characterization Center, National Institute for Materials Science, 1-2-1 Sengen, Tsukuba 305-0047, Japan*

(Received 14 September 2007; accepted 13 March 2008; published online 16 April 2008)

We have developed a robust method for fabricating Si nanoregions in silica glass using femtosecond laser processing. We attained a vivid formation of silicon-rich nanoregions site-selectively generated in SiO₂ by irradiation of femtosecond laser pulses to the interface of a SiO₂ substrate and deposited aluminum (Al) thin film, where the Al element acts as a gettering site for O atoms. Growth of high-density Si nanocrystals and amorphous Si was observed by transmission electron microscopy in the region that was multiply irradiated with the femtosecond laser. Furthermore, local annealing with a cw laser enhances the Si nanocrystal growth, which was determined by micro-Raman measurements. © 2008 American Institute of Physics. [DOI: 10.1063/1.2905289]

Silicon dioxide (SiO₂) obtained by oxidation of Si has been widely used because of its usefulness in materials such as insulator for Si devices and optical lens. Fabricating nanometer-scale local oxidation of Si has been investigated using an atomic force microscope¹ and Si nitride islands² in order to develop the fabrication process of next-age Si devices such as the quantum effect devices.³ On the other hand, local deoxidization of SiO₂ is also expected to advance Si device technology. For the technology of material processing, the development of site-selective deoxidization of SiO₂ leading to the formation of Si nanostructures is needed for the fabrication of micro- to nanoscale Si structures, such as line and pillar structures in Si nanoelectronics. Deoxidization of SiO₂ has been examined using irradiation with a focused electron beam method⁴ and an electrochemical treatment method.⁵ The electron beam method can be used only in high vacuum for the deoxidization of thin SiO₂ films on Si substrates. When the electrochemical treatment is used, deoxidized sites cannot be selected.

A focused femtosecond laser irradiation method is a strong candidate for controlling deoxidization sites of the bulk SiO₂. In fact, oxygen-deficiency defects, or E' centers are known to be formed in SiO₂ as a result of the lattice relaxation process after multiphoton absorption of femtosecond-laser light.⁶ Optical waveguides⁷ and photonic crystals⁸ have also been fabricated in SiO₂ by femtosecond-laser irradiation with micrometer accuracy. However, use of femtosecond-laser irradiation is not solely suitable for segregating Si regions in the SiO₂.⁶

It has been known that deoxidization of SiO₂ leads to the formation of alumina (Al₂O₃) and Si,^{9,10} when aluminum (Al) comes in contact with SiO₂ at a temperature above

500 °C. Furthermore, syntheses of Si nanocrystals (nc-Si's) in the SiO_x matrix are enhanced by the gettering of oxygen atoms from SiO_x caused by Al doping.¹¹

Therefore, for future Si nanoelectronics, investigating whether a similar reaction takes place at the interface between the SiO₂ substrate and Al thin film under femtosecond-laser irradiation is important in order to effectively form nanoscale Si regions in SiO₂ with a controlled structure. In this paper we demonstrate the site-selective deoxidization of SiO₂ to form localized Si regions using a combination method of both femtosecond-laser irradiation and deoxidization by Al. Structural alterations of the irradiated region were observed by transmission electron microscopy (TEM) and micro-Raman scattering. The following local laser annealing of the femtosecond-laser irradiated region was observed in situ by Raman scattering.

The SiO₂ substrate (3 × 12 × 1 mm³) was used as a laser target after deposition of Al thin film (1.4 μm) using Ar-ion sputtering. Femtosecond seed pulses from a Ti:sapphire laser oscillator, operating at a wavelength of 800 nm with a pulse duration of about 100 fs, was amplified to 5 μJ/pulse in a 100 kHz regenerative amplifier system. After compensation of the amplifier dispersion, pulses of 140 fs in duration were obtained. A laser pulse with a power of 390 mW was focused on the SiO₂ substrate near the interface of Al/SiO₂ through an objective lens (×50), as shown in Fig. 1. The energy fluence was estimated to be approximately 16.8 J/cm², which produced a SiO_x region with a high reflective index.⁸ We fabricated the SiO_x region with a line shape length of 4.5 mm by scanning the femtosecond laser with a speed of 0.05 mm/s. A focused point was estimated to be irradiated with ~4 × 10³ femtosecond-laser shots. Figure 2 shows a typical top view, optical image of the drawn lines. The widths of the drawn lines, corresponding to the produced SiO_x region, are estimated to be in a range of 2.0–2.5 μm. After femtosecond-laser irradiation, we found no ablation

^{a)}Present address: Nanodevice Innovation Research Center, National Institute of Advanced Industrial Science and Technology, 1-1-1 Higashi, Tsukuba, Ibaraki 305-8562, Japan.

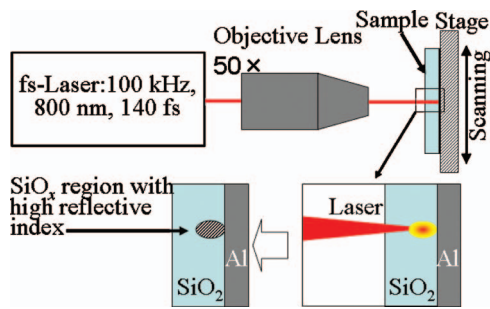


FIG. 1. (Color) Illustration of femtosecond-laser irradiation system. Femtosecond laser was focused on SiO₂ substrate near Al/SiO₂ interface and scanned to draw line structures.

damage in the deposited Al film, which indicated that the femtosecond laser was focused on the SiO₂ substrate near the Al/SiO₂ interface.

To investigate structural alterations of the SiO₂ caused by multiple femtosecond-laser irradiations, we observed a cross section of the SiO_x region by TEM. The Al layer was removed from the SiO₂ substrate by chemical etching using HCl (36%, 30 min) before TEM. Epoxy resin was deposited on the surface of the substrate to make the cross section of the TEM sample. The interface of the epoxy layer and SiO₂ corresponds to the Al/SiO₂ interface. Figure 3(a) shows the structural alterations resulting from multiple femtosecond-laser irradiations. The altered region reached $\sim 0.5 \mu\text{m}$ at the maximum depth from the Al/SiO₂ interface. Figures 3(b)–3(d) show elemental mapping obtained by energy dispersive x-ray spectrometer (EDS) elemental mapping. We found a very characteristic structure that can be formed by multiple femtosecond-laser irradiations. (i) The Si-rich $\sim 0.1\text{-}\mu\text{m}$ thick region was formed near the Al/SiO₂ interface. (ii) The Al atoms were distributed all over the altered region, not only in the Si-rich region. (iii) Concentration of O atoms gradually decreased toward the interface in the altered region, while no changes in O concentration were seen in the SiO₂ regions deeper than $\sim 0.5 \mu\text{m}$. The Si-rich region is formed by a phase separation of Si and Al and Al–O composition, and by a migration of O atoms from SiO₂ to the Al film. A higher temperature region was formed into the SiO₂ side, but not at the Al film side because the focused point in the SiO₂ was femtosecond-laser irradiated from the SiO₂ side, as shown in Fig. 1. Since a melting point of Al (660 °C) is much lower than that of SiO₂ (1710 °C), the Al regions are effectively solidified in the higher temperature region during the repeated phase changes induced by femtosecond-laser irradiation. As a result, the Al-rich region is probably generated in a deeper place than in the Si-rich region.

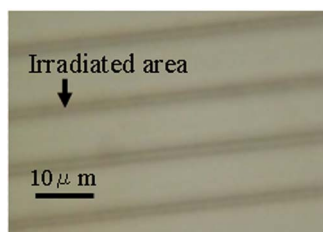


FIG. 2. (Color online) Optical image of drawn lines formed inside SiO₂ substrate near Al/SiO₂ interface by femtosecond-laser scanning with $\sim 4 \times 10^3$ shots.

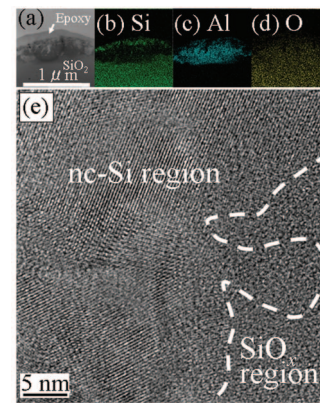


FIG. 3. (Color) Bright-field cross-section scanning TEM images (a) of Al-doped SiO_x region by femtosecond-laser irradiation and corresponding EDS elemental mapping of (b) Si, (c) Al, and (d) O. (e) TEM image of nc-Si's in SiO_x matrix near epoxy resin and SiO_x interface. Dashed line shows boundary between nc-Si and SiO_x regions.

During the high resolution (HR-) TEM observation we observed a dense formation of nc-Si's in the Si-rich region, as shown in Fig. 3(e). The Si lattice planes are clearly visible with several orientations in the HR-TEM image. These lattice planes have an interplane distance of approximately 3 Å. The nc-Si's are stacked up in the HR-TEM image. The single-domain size of the nc-Si's were estimated to be approximately 5–20 nm. This shows that the presence of Al atoms enables the deoxidization of SiO₂ and the formation of nc-Si's by femtosecond-laser irradiation. The Al atoms act as a gettering site for O atoms, which are released from SiO₂ by femtosecond-laser irradiation.

Figure 4 shows Raman spectra obtained from the femtosecond-laser irradiated area of the SiO₂ where a 532 nm green cw laser with a power of 0.014–14 mW was focused on the sample at $\sim 1 \mu\text{m}$ in diameter to excite it. These spectra were taken from the same position on the sample. During 0.014 mW irradiation, we found the Si optical phonon peak at 516–518 cm⁻¹ in the spectrum, which is lower than the well-known frequency of the Raman band from crystalline bulk Si, i.e., 520.1 cm⁻¹. The Raman band has an asymmetric line shape and a broad full width at half maximum (FWHM) of 15–16 cm⁻¹. These lowered Raman peak values and the asymmetrical broadening seem to be a result of phonon confinement in the nc-Si.^{12,13}

When the laser power was increased to 0.14 mW, broad peaks at ~ 300 and 460–480 cm⁻¹ from amorphous Si (*a*-Si)¹⁴ were clearly observed in the spectrum. This indicates that the *a*-Si region was generated by cw laser irradiation. We observed a robust crystalline Si band at ~ 508 cm⁻¹, indicating that crystallization of the *a*-Si region was enhanced by increasing the laser power to 1.4 mW. Furthermore, the crystallization was strongly augmented by laser irradiation with a higher power of 14 mW at which we observed a sharp crystalline Si band of 493 cm⁻¹ and a decrease in intensity of the *a*-Si signal. An observed downshift of the Si phonon frequency was enhanced by increasing the laser power. Quantitative estimation of the lattice temperature of nc-Si during laser irradiation was performed using a Raman shift of the Si optical phonon.¹⁵ This estimation reveals $T \sim 900$ K for the irradiated laser power of 1.4 mW and $T \sim 1300$ K for 14 mW, corresponding to the power density of 1.8×10^5 and 1.8×10^6 W/cm², respectively.

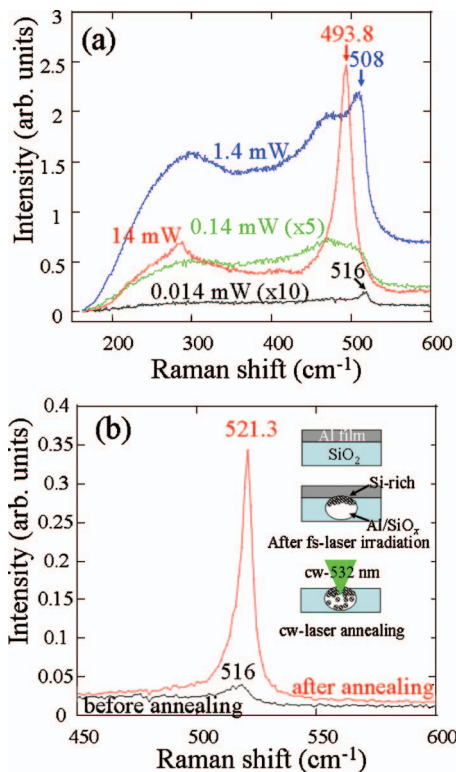


FIG. 4. (Color) Microscopic Raman scattering spectra from femtosecond-laser irradiated region. (a) Raman spectra measured using different excitation power (0.014–14 mW) with 532 nm cw laser. These Raman spectra were obtained by integrating 120 s for 0.014–1.4 mW and 2 s for 14 mW. (b) Comparison of Raman spectra before and after 523 nm cw laser irradiation with 14 mW. Illustrations of structure alteration using cw laser irradiation are shown as inset.

To investigate phonon properties of the crystallized Si region, we measured the Raman spectra with the lowest laser power of 0.014 mW, followed by laser annealing with 14 mW irradiation. The Raman intensity of the Si phonon band increased up to 25 times, as shown in Fig. 4(b), as a result of the laser annealing. An asymmetrical broad peak, which has a FWHM value of 6 cm^{-1} , shows that the Si optical phonon originated from the nc-Si's. An increase in the Raman intensity thus indicates that nc-Si's were generated from *a*-Si regions in the SiO_x region by laser annealing. We noted that the Raman scattering was usually observed at $520\text{--}521 \text{ cm}^{-1}$ in crystalline Si, while a lowering of the phonon frequency to less than 520 cm^{-1} was observed before the laser annealing. Such a difference is attributed to the growth of the nc-Si's and presence of a compressive stress¹⁶ generated in the nc-Si's after the laser annealing.

To understand the crystallization dynamics statistically, we performed the laser annealing at more than 20 positions with a laser power density of $1.1 \times 10^5\text{--}1.8 \times 10^6 \text{ W cm}^{-2}$. Figure 5 shows a summary of the laser power dependences of the averaged intensity of the Si optical phonon before and after the 2.0 s laser irradiation and the Raman shift during the laser annealing. The Raman intensity increased with the laser power density. The laser-irradiation-induced generation of nc-Si's occurred in the laser power density range of 3.0×10^5 to $1.8 \times 10^6 \text{ W cm}^{-2}$. The threshold of crystallization of *a*-Si dots was located between 1.8×10^5 and $3.0 \times 10^5 \text{ W cm}^{-2}$. A downshift of the Raman shift, which indi-

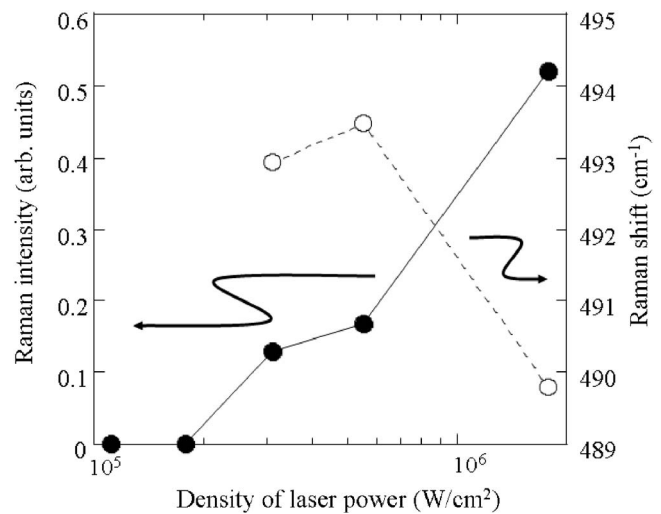


FIG. 5. Increment of Raman peak intensity (closed circles) of Si optical phonon after 532 nm cw laser irradiation, depending on power density of $1.1 \times 10^5\text{--}1.8 \times 10^6 \text{ W cm}^{-2}$ and Raman shift of Si optical phonon during cw laser irradiation (open circles).

icates an increase in nc-Si temperature, was enhanced by increasing the laser power density to $1.8 \times 10^6 \text{ W cm}^{-2}$.

In conclusion, the nc-Si and *a*-Si regions were formed in SiO_2 by femtosecond-laser irradiation at the interface between SiO_2 and Al thin film. Crystallization of the *a*-Si regions was enhanced by 532 nm cw laser annealing with a power density of 3.0×10^5 to $1.8 \times 10^6 \text{ W cm}^{-2}$. Results of TEM and Raman measurements show that the nc-Si's were generated with a high density. This means that the method using the deoxidization effect of Al and femtosecond-laser irradiation is a useful means of microfabricating Si structures consisting with nc-Si's in SiO_2 .

A part of this work was supported by the Nanotechnology Support Project of the Ministry of Education, Culture, Sports, Science and Technology (MEXT), Japan.

- ¹Y. Y. Wei and G. Eres, *Appl. Phys. Lett.* **76**, 194 (2000).
- ²M. Tabe and T. Yamamoto, *Appl. Phys. Lett.* **69**, 2222 (1996).
- ³A. Zaslavsky, C. Aydin, S. Luryi, S. Cristoloveanu, D. Mariolle, D. Fraboulet, and S. Deleonibus, *Appl. Phys. Lett.* **83**, 1653 (2003).
- ⁴B. Carriere and B. Lang, *Surf. Sci.* **64**, 209 (1977).
- ⁵T. Nohira, K. Yasuda, and Y. Ito, *Nat. Mater.* **2**, 397 (2003).
- ⁶N. Fukata, Y. Yamamoto, K. Murakami, M. Hase, and M. Kitajima, *Appl. Phys. Lett.* **83**, 3495 (2003).
- ⁷K. Miura, J. Qiu, H. Inouye, T. Mituyuu, and K. Hiramno, *Appl. Phys. Lett.* **71**, 3329 (1997).
- ⁸Y. Xu, H. B. Sun, J. Y. Ye, S. Matuo, and H. Misawa, *J. Opt. Soc. Am. B* **18**, 1084 (2001).
- ⁹L. Balazs, V. Fleury, F. Duclos, and A. Van Herpen, *Phys. Rev. E* **54**, 599 (1996).
- ¹⁰J. P. Blondeau, L. Allam, V. Fleury, P. Simon, and I. Gregora, *Mater. Sci. Eng., B* **100**, 27 (2003).
- ¹¹N. Uchida, T. Okami, H. Tagami, N. Fukata, M. Mitome, Y. Bando, and K. Murakami, *Physica E (Amsterdam)* **38**, 31 (2007).
- ¹²T. Okada, T. Iwaki, H. Kawashima, and K. Yamamoto, *J. Phys. Soc. Jpn.* **54**, 1173 (1985).
- ¹³S. Piscanec, M. Cantoro, A. C. Ferrari, J. A. Zapien, Y. Lifshitz, S. T. Lee, S. Hofmann, and J. Robertson, *Phys. Rev. B* **68**, 241312(R) (2003).
- ¹⁴D. Bernejo and M. Cardona, *J. Non-Cryst. Solids* **32**, 405 (1979).
- ¹⁵V. Poborchii, T. Tada, and T. Kanayama, *J. Appl. Phys.* **97**, 104323 (2005).
- ¹⁶L. Khriachtchev, M. Räsänen, and S. Novikov, *Appl. Phys. Lett.* **88**, 013102 (2006).